1

Introduction

Field-effect transistors (FETs) are developed using various semiconductor materials, the most common of which is silicon (Si). FETs are employed in many products and lead to performance improvements and reductions in size and weight, with increasing miniaturization. The extraordinary progress in the Si FET technology used in both large-scale integrated circuits (LSIs) and flat-panel displays has a tremendous impact on lifestyles. Several players continue to be engaged in the fierce race to further develop Si FET technology. Meanwhile, device power consumption continues to increase, and lowering the power consumption has become necessary for various applications, such as the Internet of Things (IoT) and wearable applications.

Given these circumstances, crystalline oxide semiconductors (crystalline OS) draw much attention for their ability to reduce power consumption in electronic circuits. IGZO has been particularly studied in detail, and its fundamental properties have been examined to develop its applications for products. The discovery of a unique class of crystalline OS, the *c*-axis-aligned crystalline IGZO (CAAC-IGZO), is a key finding of these studies.

Physics and Technology of Crystalline Oxide Semiconductor CAAC-IGZO documents the research and developments reported by S. Yamazaki and colleagues to date. It consists of three volumes, namely *Fundamentals*, *Application to LSI*, and *Application to Displays* (Figure 1.1). *Fundamentals* introduces oxide semiconductor materials, crystal structure analysis, the fundamental properties and FET characteristics of CAAC-IGZO, and a comparison with Si FETs [1]. *Application to LSI* focuses on the applications of CAAC-IGZO to LSI devices, and describes the FET structures, fundamental electrical characteristics, nano-sized (e.g., 20-nm node) transistor prototypes, and examples of LSI applications, including non-volatile memory devices [2].

This volume, entitled *Application to Displays*, introduces approaches to fulfill the market demand for devices with further enhancements in image displays at lower costs and power

Physics and Technology of Crystalline Oxide Semiconductor CAAC-IGZO: Application to Displays, First Edition.
Edited by Shunpei Yamazaki and Tetsuo Tsutsui.

Figure 1.1 Framework of *Physics and Technology of Crystalline Oxide Semiconductor CAAC-IGZO*

consumption. In particular, it describes the CAAC-IGZO FET structure, manufacturing processes, FET characteristics, and circuit design. Subsequently, the organic light-emitting diode (OLED) display, a highly promising next-generation technology, is presented. In particular, the materials and elements for power-efficient operations are discussed in detail, along with the pixel structures for high-yield displays with a high pixel density.

This volume also introduces the fabrication method of flexible displays based on OLED displays, and proposes new possibilities for displays, sensors, and other devices. In addition, it presents a review of liquid crystal displays (LCDs), which are currently the most popular displays, from the point of view of providing high resolution and low power consumption.

Furthermore, the volume also discusses actual OLED displays with CAAC-IGZO FETs, LCD circuit designs, and display prototypes with a high pixel density.

1.1 History of Displays

For more than half a century, cathode-ray tubes (CRTs) were used to develop display devices for televisions (TVs) and monitors. However, the development and widespread use of LCDs [3] has replaced CRTs as they produce flat-panel displays that are thin, light, and have low power consumption. The earliest LCDs used in watches and calculators displayed monochrome alphanumeric characters in a small display area. Then, larger LCDs were developed and used in word processors, which displayed more characters and pictures. This was followed by laptop computers, which displayed more detailed color images. Next, pagers – as portable personal terminals – attracted the attention of companies and students, but were swiftly replaced by mobile phones. The first mobile phones could only display alphanumeric characters. Subsequently, mobile phones were developed to include integrated cameras capable of handling images, mapping data, and downloading audiovisual information from the Internet. As a result, larger color displays with an increased number of pixels appeared and resulted in displays with higher pixel densities.

The increasing number of pixels forced the LCDs to abandon a passive-matrix-driving method in favor of active-matrix (AM) driving [4], by incorporating a storage capacitor and thin-film transistors (TFTs) in each pixel. Additionally, the video display required a shorter display refresh period and this was another reason for the introduction of AM LCDs. The passive-matrix driving was slow, because of both the liquid crystal material response and the duty driving that could not retain the amount of rewriting required for gate lines in a limited period. There was also a limit on reducing the distance between pixels, because of the crosstalk between adjacent pixels. AM displays were popular, as they allowed high-speed refresh for video portrayal, because of the direct writing of video data into the storage capacitor through the pixel FET. Hence, fast data rewriting was possible even for a significantly large number of pixels without the need to wait for the refresh to complete. AM LCDs also ensured a large number of gray shades and high contrasts, because the gray levels were completely stored as an analog amount of charges written in the storage capacitor.

With the coming of the 21st century, large CRT TVs were eventually replaced by AM LCD TVs. Simultaneously, TV broadcasting moved from analog to digital, and full high-definition TVs (1920×1080) were widely adopted by the market. Currently, 4 K TVs (3840×2160), which are compatible with 4 K broadcasting, are being developed in mainstream markets. They will shortly be succeeded by 8 K broadcasting and 8 K TVs (7680×4320) [5, 6].

1.2 Requirement for Displays

Early AM LCD TV displays exhibited motion blurring as a result of the sample-and-hold addressing. Hence, many LCDs adopted black frame insertion (BFI) between video frames and/or backlight blinking to solve the problem of blurring. A refresh rate higher than 50/60 Hz, similar to CRTs, is thereby required to avoid flicker, which disappears at approximately 75–85 Hz. However, the broadcasting and video standards were sampled at 50 or 60 Hz (25 or 30 Hz interlaced) to avoid image tearing by doubling the chosen refresh rate, particularly in the case of 50 Hz CRTs. The AM LCDs with BFI or backlight blinking similarly doubled the refresh rate. Frame interpolation with constant backlight and without BFI was introduced, as they faced the issue of reduced luminance. Some products even adopted quadruple refresh rates.

To date, the pixel FETs in large displays, such as TVs and monitors, use amorphous silicon (a-Si) because of the mass-manufacturing compatibility for large glass substrates [7]. Unfortunately, the a-Si TFTs have low mobility and are not compatible with high-speed data writing in large screens with high resistive/capacitive (RC) loads. Therefore, the pixel numbers required for full high definition (1920×1080) are barely manageable with a-Si TFTs. Hence, other FET technologies are required for 4 K (3840×2160) and 8 K (7680×4320) displays, which exhibit much higher RC loads. Various attempts were made to reduce the loads. Examples of these include introducing copper wirings, dividing the driving by splitting the screen horizontally or vertically, inserting black frames by synchronizing the partition control of the backlights, and rewriting the image data. However, these approaches resulted in increased costs and also increased the power consumption of the control ICs and backlights.

The development of both cable and wireless Internet networks allows individuals to ubiquitously access information. This facilitated the transition from mobile phones to smartphones, and from laptops and desktop computers to tablet computers. The development of devices and infrastructures that could handle large amounts of data, such as high-bandwidth videos, has also contributed to this situation. Additionally, touch sensors revolutionized the human–machine interface (HMI) through increased interactivity. This also necessitated high-performance display devices.

For personal displays for virtual reality (VR) and augmented reality (AR) applications, the pixel density, cost, and power consumption are extremely challenging issues, particularly for the 8K format, so new solutions are necessary. There is also a growing trend of curved displays in, for example, automotive applications.

The key quality factors for high-performance displays include high contrast, excellent color reproduction, high resolution, and crisp and flicker-free moving images. In particular, displays viewed at a short distance require high resolution to avoid jaggedness.

The requirements for these displays depend on their use case and screen size. Small-display personal devices require particularly high pixel density and smaller FETs. For example, a pixel density of over 1000 PPI (for VR and AR applications) requires FETs with a channel length as short as 2–3 μm. This size cannot be achieved even by low-temperature polysilicon (LTPS), which is a FET technology widely used in current small-sized displays. Furthermore, the increase in the number of pixels also increases the number of gate lines and pixel data lines. Hence, higher-performance FETs are necessary in the driving and control circuits integrated on the display substrate. For example, when a display panel is synchronized with a touch sensor, a part of the display period is allocated to the sensor driving and read-out. Thus, the control FETs are required to be smaller and to be operated at higher speeds and higher currents. This in turn

necessitates high mobility and on-state current. The small FETs also ensure a higher aperture ratio, which leads to a lower total power consumption for a given display luminance.

The above discussion is mainly applicable for LCDs, which are common display devices. However, it is also important to focus on OLED displays, which constitute the next-generation displays already being mass produced by some manufacturers. The FETs for OLED displays require higher performances than those of LCDs, as they are driven by current.

Although large-sized and medium-sized LCD TVs and monitors still use a-Si TFTs, they are unable to sustain the increasing RC loads associated with the higher pixel counts and refresh rates. This problem was addressed by increasing the circuit scale and/or using division driving or other methods. However, this increased the cost and power consumption. Therefore, a-Si TFTs in these devices should be replaced by oxide semiconductor FETs. The currently mass-produced OLED TVs also use oxide semiconductor FETs because of their good current uniformity and compatibility with large-sized manufacturing.

LTPS TFTs are unsatisfactory for use in small displays with ultra-high pixel density. This will be discussed in detail later in this volume. They also face a challenge in the mass production of large displays.

This volume explains the reasons why CAAC-IGZO FETs can be applied to a wide range of displays (from large TVs to small displays with high pixel densities), as well as to circuit technologies of the displays using them. It also describes a fabrication technology for small and large foldable displays and the development of an apparatus for this purpose.

1.3 Transistor Technology for Displays

Various devices using flat-panel displays, such as TVs and smartphones, are widespread and indispensable in our daily life. The current mainstream flat-panel displays are LCDs. As next-generation displays, OLED displays are actively being developed by an increasing number of organizations [8]. Traditionally, hydrogenated amorphous silicon (a-Si:H) TFTs were widely employed for LCD TVs and monitors as switching elements.

As the demand for higher-performance display panels increases, FETs (in the following description, there are cases where the term "FETs" includes "TFTs") with higher driving capability are required. This has led to the development of LTPS by several manufacturers [9–12]. However, since LTPS is fabricated by crystallizing a-Si, expertise is required to control the crystallization process. Furthermore, the application of LTPS to larger substrates is considered to be difficult compared with a-Si:H.

Recently, the use of oxide semiconductors as FETs has drawn much attention [13]. As mentioned in this book series, this class of semiconductor materials is remarkably different from Si; they have driving capabilities lower than that of LTPS but higher than that of a-Si:H. Oxide semiconductors are also characterized by their applicability to large substrates and relaxed fabrication requirements, such as low process temperatures and easy etching. Unlike LTPS, they do not require laser annealing, which is expensive and difficult for large substrates.

Oxide semiconductors offer an advantage in the form of higher driving capabilities but formerly had a disadvantage in the instability of the film formation and device characteristics compared with a-Si:H. Yamazaki and co-workers discovered crystalline IGZO (i.e., CAAC-IGZO; for more details, see [1]). This has a small film-defect density, enabling the fabrication of FETs with a short channel length, and thereby extending their applicability to high-resolution

displays. CAAC-IGZO provides unique characteristics, including extremely low off-state current, compared with the widely used Si. This will be described in detail later.

This section reports on the process and characteristics of CAAC-IGZO FETs for display applications compared with those of Si.

1.3.1 Comparison of Silicon and Oxide Semiconductors

This subsection compares a-Si:H, LTPS, and IGZO. In terms of the FET fabrication process, a-Si:H is the shortest and contains fewer steps, followed by CAAC-IGZO, and LTPS is the longest. It is critical to reduce the number of process steps and their complexity to maximize the manufacturing yield. LTPS has a more extensive process than those of a-Si:H and CAAC-IGZO, as it requires the linear-beam laser crystallization of Si, high-temperature annealing, and ion doping. LTPS also has the disadvantage of expensive plant and equipment investment, because it requires special apparatus and expensive ion doping. The linear-beam laser equipment is also difficult to fabricate, especially for a large substrate such as G8. In contrast, a-Si:H and CAAC-IGZO technologies do not need any special apparatus, and are thus easily applicable for large substrates.

Semiconductor Energy Laboratory Co., Ltd. (SEL) initiated the development of linear-beam laser equipment (Figure 1.2) [14–17]. This was undertaken by equipment manufacturers in a widespread manner and is now indispensable for LTPS crystallization. The linear-beam laser equipment was initially developed for element separation in the modularization of solar cells. After using the linear-beam laser equipment for LTPS, SEL then researched CAAC-IGZO, with its high uniformity and large substrate capability.

Figure 1.2 Linear-beam laser equipment developed by SEL. *Source*: Reproduced from [17]. Copyright (2014), with permission from Wiley

Table 1.1 Substrate size class and intended use of a-Si:H, LTPS, and IGZO

	Resolution	a-Si:H	LTPS	CAAC-IGZO
Large TV	Higher	Fair	Poor	Good
(60 inch or more)	Lower	Good	Poor	Good
Medium TV	Higher	Good	Poor	Good
(20–55 inch)	Lower	Good	Poor	Good
Small and medium panel for tablet computers	Higher (4K2K)	Fair	Good	Good
(up to 10 inch)	Medium (FHD)	Good	Good	Good
	Lower (HD)	Good	Good	Good
Small and medium panel for smartphones	Higher (4K2K)	Fair	Good	Good
(up to 6 inch)	Medium (FHD)	Fair	Good	Good
	Lower (HD)	Good	Good	Good

Increasing the substrate size significantly contributed to lowering unit fabrication costs, as a larger substrate could yield a larger number of display panels. Table 1.1 lists some classes of substrate size intended for use in display manufacturing, and the potential for achieving high-resolution displays by employing silicon and oxide semiconductors. As described above, a-Si:H and CAAC-IGZO do not need any special equipment; thus, they could readily be applied to large substrates up to the tenth generation mother-glass size (approximately 3 m square). This allows the manufacture of large-sized TVs mainly by using LCD backplanes fabricated from a-S:H TFTs. Recent advances in the development of CAAC-IGZO have demonstrated that it also enables large TV fabrication. Additionally, it exhibits higher FET performance compared with a-Si:H, thereby enabling gate driver integration even for large TVs with high resolutions.

Large mother glasses also enable the manufacture of small-sized and medium-sized display panels in large volumes for smartphones and tablet computers. High resolution is a key factor for such panels, and requires increasing the FET driving capability. To date, LTPS with higher FET performance compared with a-Si:H was used for small and medium panels with high resolutions. Nevertheless, some aspects of the performance of CAAC-IGZO FETs are comparable with that of LTPS TFTs for small-sized and medium-sized panels. Therefore, CAAC-IGZO could be regarded as a prospective material for the production of display panels in a wide range of sizes and for various uses.

Figure 1.3 shows the FET characteristics of silicon and oxide semiconductors. FETs with silicon as an active layer exhibit a high off-state current, whereas the CAAC-IGZO FET exhibits an off-state current lower than the detection limit of the measurement apparatus. The low power consumption is an important characteristic for Displays. Applications utilizing the low off-state current will be described in Chapter 6 and elsewhere.

Table 1.2 compares silicon and oxide semiconductors in terms of manufacturability. Liquid crystal panels could be fabricated with almost the same number of masks as that of a-Si:H by using CAAC-IGZO [18, 19]. As the FET performance of CAAC-IGZO is higher than that of a-Si:H, it permits the narrowing of the bezels by integrating the gate driver on the panel (GOP), even in high-resolution displays [20]. The CAAC-IGZO FETs have an off-state current on the order of yoctoamps per micrometer (yA/μm) (where $y = 10^{-24}$) compared with femtoamps per micrometer (fA/μm) (where $f = 10^{-15}$) for LTPS TFTs and a-Si:H TFTs. As a result, it enables low-frequency display refresh and an associated lower power consumption (the panel driving power is proportional to the refresh frequency). This feature is also known as idling-stop (IDS) driving. IDS driving is a method for reducing power consumption for displays by showing

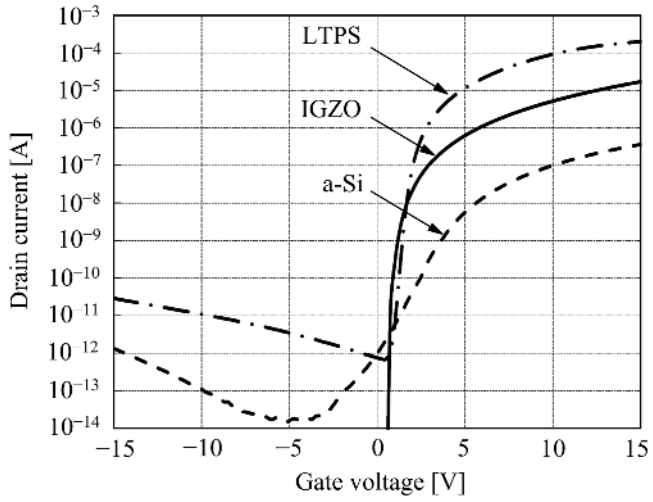

Figure 1.3 FET characteristics with an active layer of each semiconductor

Table 1.2 Comparison of a-Si:H, LTPS, and CAAC-IGZO. *Source*: Reprinted from [18, 19]. Copyright (2015), with permission from Wiley

	a-Si:H	LTPS	CAAC-IGZO
Number of masks for fabricating LCD (for FET only)	5–8 (4)	8–12 (5)	6–8 (4)
Process temperatures	350 °C	400 °C	350 °C
Gate driver	Depends on specifications	Applicable	Applicable
Mobility	Up to 1 cm^2/V-s	Up to 100 cm^2/V-s	Up to 40 cm^2/V-s
Size of mother glass	G4.5–G10	G4.5–G6	G4.5–G10
Device costs	Low	High	Low
Plant costs	Low	High	Low

static images. This topic will be described in detail in Chapter 6. IDS driving provides a significant power advantage, particularly for always-on, reflective or transflective mobile displays.

1.3.2 FETs in LCDs

FETs are used in pixel circuits, gate drivers, and other parts of LCDs and OLED displays. The characteristics of FETs required for these devices are briefly described below.

Figure 1.4 shows a pixel circuit of LCDs. The FET in the pixel circuit is used as a switch, as described in Figure 1.5. It performs image writing and retention operations when it is turned on and off, respectively.

As shown in the timing diagram illustrated in Figure 1.6, the retention operation is executed by turning off the pixel FET so that the voltage written into the capacitor Cs remains until the subsequent write period. As mentioned, IGZO features an extremely low off-state current that

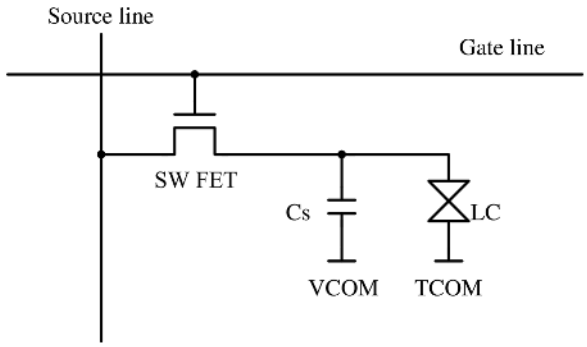

Figure 1.4 Circuit diagram of the LCD pixel

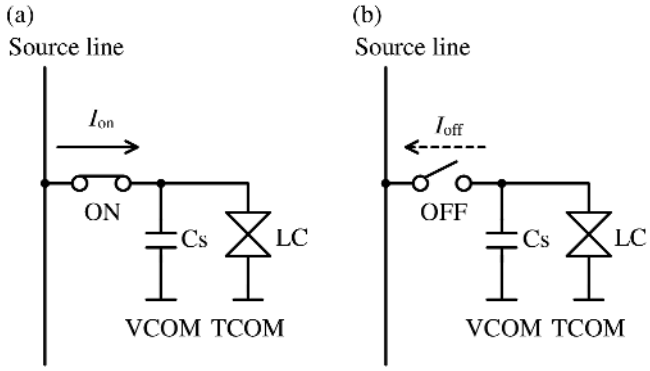

Figure 1.5 Circuit operation of LCD pixel: (a) writing operation; (b) retention operation

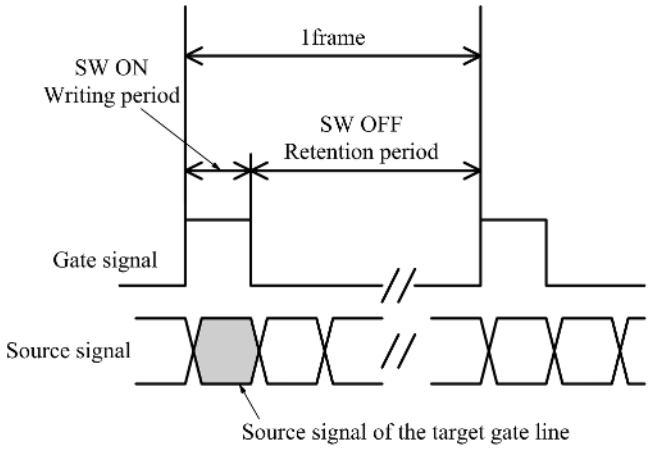

Figure 1.6 Timing diagram of gate and source signals used in the LCD pixel circuit

Table 1.3 Pixel capacitances and off-state current (allowable range of voltage shift is 20 mV)

	Required off-state current	
Capacitance per pixel	Standard driving (60 Hz)	IDS driving (1 Hz)
150 fF	1.8×10^{-13} A	3.0×10^{-15} A
15 fF	1.8×10^{-14} A	3.0×10^{-16} A

enables driving at a low refresh frequency. Table 1.3 shows the off-state current required for this type of driving. The maximum allowed off-state current depends on the storage capacitance of the pixel, and it has to be lower as the storage capacitance becomes smaller. As the resolution increases, the pixel size decreases, and hence the storage capacitor becomes small. Thus, a much lower off-state current is required for the IDS driving of high-resolution displays. In addition, the retention period is much longer than the writing period, thus, reliability is required in the off state, in which a negative voltage is applied to the gate.

The calculation conditions are as follows:

- Standard driving (60 Hz refresh rate)

$$I_{\text{off}} = 150 \times 10^{-15} \times 0.02 / \left(16.67 \times 10^{-3}\right) = 1.80 \times 10^{-13} \text{ A}.$$

- IDS driving (1 fps)

$$I_{\text{off}} = 150 \times 10^{-15} \times 0.02 / 1 = 3 \times 10^{-15} \text{ A}.$$

Next, the image data-writing operation is described. The pixel FET is turned on to write image data to a pixel. A data voltage from a source line is written to the pixel capacitor Cs. In this case, the writing of the data voltage should be completed within the writing period, as shown in Figure 1.6.

If the on-state current is sufficiently large, the time constant of the source line, which is determined by a wiring resistance and parasitic capacitance, is generally larger than that of the pixel, which is determined by the on-state resistance of the switch FET and the storage capacitance. In the case of CAAC-IGZO FET or LTPS TFT, unlike a-Si, the channel width of the switch FET is determined by the design rule, and hence a large variety of LCDs can be driven.

Furthermore, as illustrated in Figure 1.7, the FETs function as a switch in the driver circuits. Figure 1.7 shows an output part in a driver circuit. The on-state current of the FET determines the time delay of the output part in a driver circuit, as shown in Figure 1.8. Therefore, a high on-state current is required for high-frequency operations in a driver circuit. In addition, a FET with large on-state current is necessary because the gate line has a large load capacitance. A method to increase the on-state current involves increasing the FET channel width. However, this also increases the driver circuit size, and thus the display bezel width.

As shown in Figures 1.7 and 1.8, a low off-state current is not as necessary in a driving circuit as in a pixel circuit. Nevertheless, the total power consumption of the driving circuit can be kept low by keeping this current as low as possible.

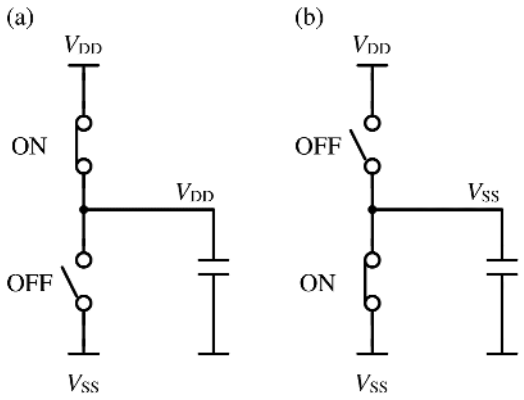

Figure 1.7 Examples of an output part in a driver circuit: (a) high output; (b) low output

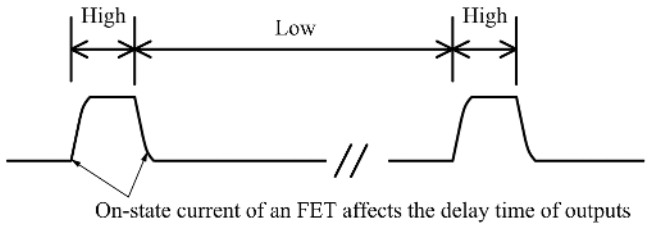

Figure 1.8 Waveform of an output from a driver circuit

1.3.3 FETs in OLED Displays

OLED displays consist of an array of self-emitting organic electroluminescent (EL) elements. Hence, unlike LCDs, they do not require any backlight source. Additionally, OLED displays could easily be made flexible. This is because the image formation is not based on optical retardation, a mechanism readily affected by even nanometer-sized changes in the display structure [21].

As shown in Figure 1.9, the OLED pixel luminance is proportional to the current per pixel. Thus, the image and display total dimming could easily be controlled. Conversely, the electro-optical transfer function of LCDs has an S-shape; thus, a look-up table (LUT) is necessary to achieve a linear response.

Driver circuits on a FET substrate for both OLED displays and LCDs comprise shift registers for selecting pixel rows. Thus, although the supply voltage is different, the *scan* or *gate*-driver circuits are almost identical. As shown in Figure 1.10, the pixel FET in an LCD functions as a *voltage* switch. In contrast, the driving FET in an OLED pixel adjusts the *current* flowing through the OLED element, which is connected serially with the driving FET (M2) [18]. This indicates that the OLED luminance also changes by degradations in the OLED element and/or driving FET, resulting in an undesired variation in the luminance across the panel. Therefore, OLED displays generally contain compensation circuits that keep the current constant by adjusting the driving voltage. However, as the degradation progresses, there is a voltage limit by which this compensation could be carried out.

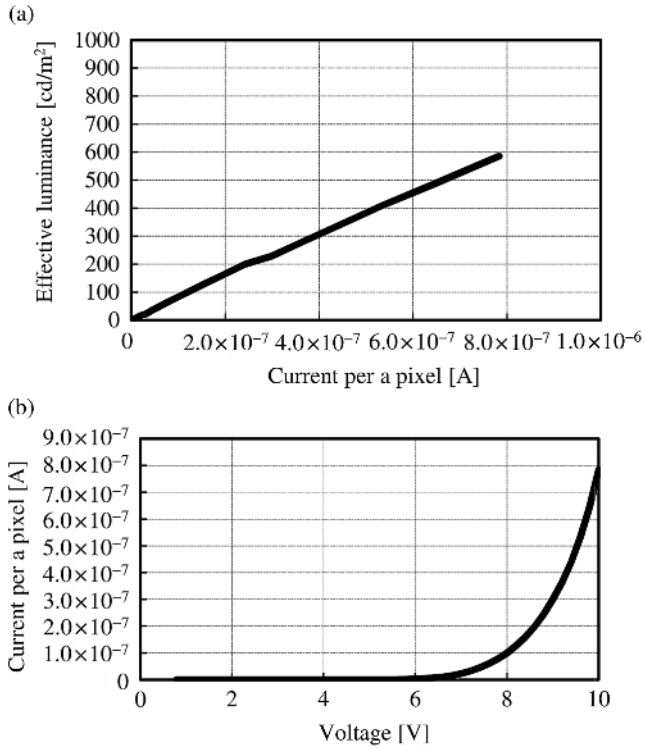

Figure 1.9 Current–effective luminance characteristics of the OLED element and voltage–current characteristics (blue element)

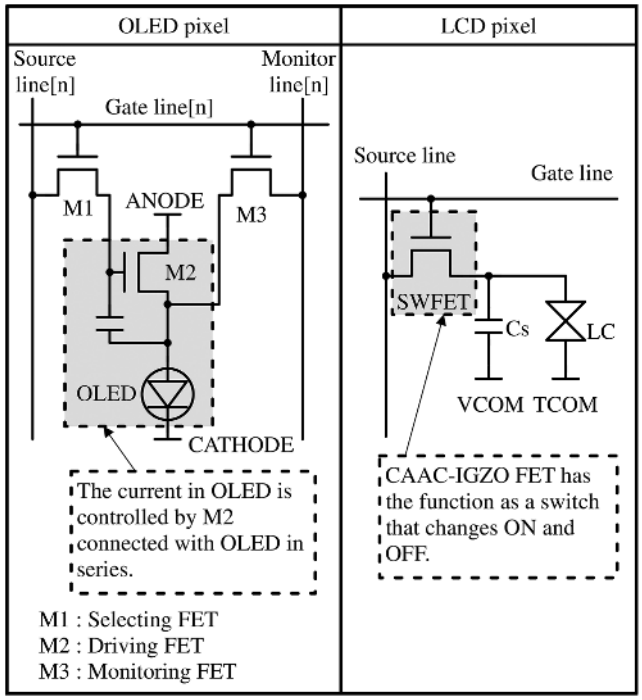

Figure 1.10 Examples of the pixel circuit configurations of OLED display (left) and LCD (right)

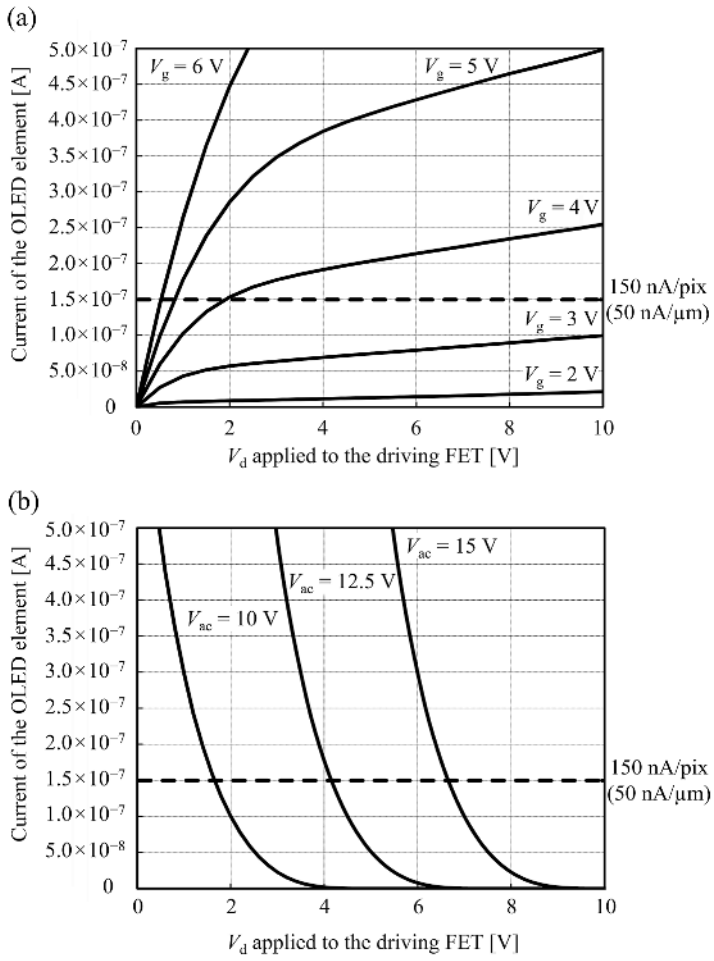

Figure 1.11 I_d–V_d characteristics of the driving FET (a) and I–V characteristics of the OLED element (b). FET characteristics: $L/W = 6/3$ μm, EL characteristics: blue element

V_d can be expressed by as follows:

$$V_d = V_{ac} - V_{el}, \tag{1.1}$$

where

V_d = voltage between the source and drain of the driving FET
V_{el} = voltage drop across the OLED element
V_{ac} = voltage between the OLED cathode and the drain of the driving FET.

Therefore, V_d of the driving circuit is adjusted according to the changes in OLED element resistance associated with its degradation.

As shown in Figure 1.11, the light emission from the OLED element in an OLED display depends on the *I–V* characteristics of both the driving FET and OLED elements. The intersection between the two *I–V* curves gives the current value for light emission. The OLED element emits light proportional to the current value.

Accordingly, the current flowing through the driving transistor (and OLED element) decreases as a result of degradation [downward shift in Figure 1.11(a)], that is, a shift in V_d. Furthermore, the luminance and anode/cathode voltage is reduced accordingly, as indicated by a leftward shift in Figure 1.11(b).

It is important to use the anode/cathode voltage in the *I–V* saturation region of the driving FET to minimize the influence of V_d reduction by degradation of the OLED element. Therefore, the saturation characteristics (current independent of the voltage) of the driving FET are important.

From the above discussion, the following three features of driving FETs are considered necessary.

1. Constant current characteristics (saturation in I_d–V_d characteristics).
2. Reduction in spatial current variation (especially variation between adjacent pixel FETs).
3. Stability over time (such as drain current variation resulting from current stress).

1.3.4 Recent FET Technologies

LCD and OLED display backplanes with various CAAC IGZO materials and FET structures were developed and evaluated to obtain the three previously discussed features. Figures 1.12–1.14 show comparisons of the *I–V* characteristics, on-state currents, *S*-values of several types of CAAC-IGZO, and commercialized LTPS TFTs. The CAAC-IGZO FETs have a top-gate self-aligned (TGSA) structure, which will be introduced in Section 2.3. It should be noted that "nIGZO" and "sIGZO" in the figures are new materials, which will be described in detail in Section 2.4: nIGZO is a high-mobility CAAC-IGZO and sIGZO is a material that exhibits further higher mobility than nIGZO [22].

Even with a channel length of $L = 2$ μm, the sIGZO FET exhibits improved on-state current (the field-effect electron mobility was approximately 60 cm^2/V-s). This was equivalent to the mobility of the commercialized LTPS TFT ($L \approx 6.4$ μm). Simultaneously, the sIGZO FET maintained the normally-off characteristics of nIGZO. The *S*-value of the sIGZO FET was approximately half that of the LTPS TFT. This indicated that it was more suitable for low-voltage driving compared with LTPS TFTs.

Figure 1.15 shows the results of gate bias temperature (GBT) stress tests. As shown, the change in threshold voltage as a result of the stress was similar for the sIGZO FET and the *p*-channel LTPS TFT in a gate driver. Details of the GBT stress test will be given in Section 2.5.

As previously mentioned, the two FET requirements for OLED display driving include the following: (1) a constant current irrespective of the changes in the drain voltage V_d; (2) a small current change from FET deterioration. As shown in Figure 1.16, the $I_d - V_d$ saturation characteristics of FETs used for driving the OLEDs were measured to evaluate both the aforementioned factors; the saturation properties of the LTPS TFT are not enough, even with a channel length of $L \approx 6.4$ μm [23]. This was attributed to a short-channel effect, and suggested that there was a limitation on scaling down the LTPS TFT size. However, the nIGZO

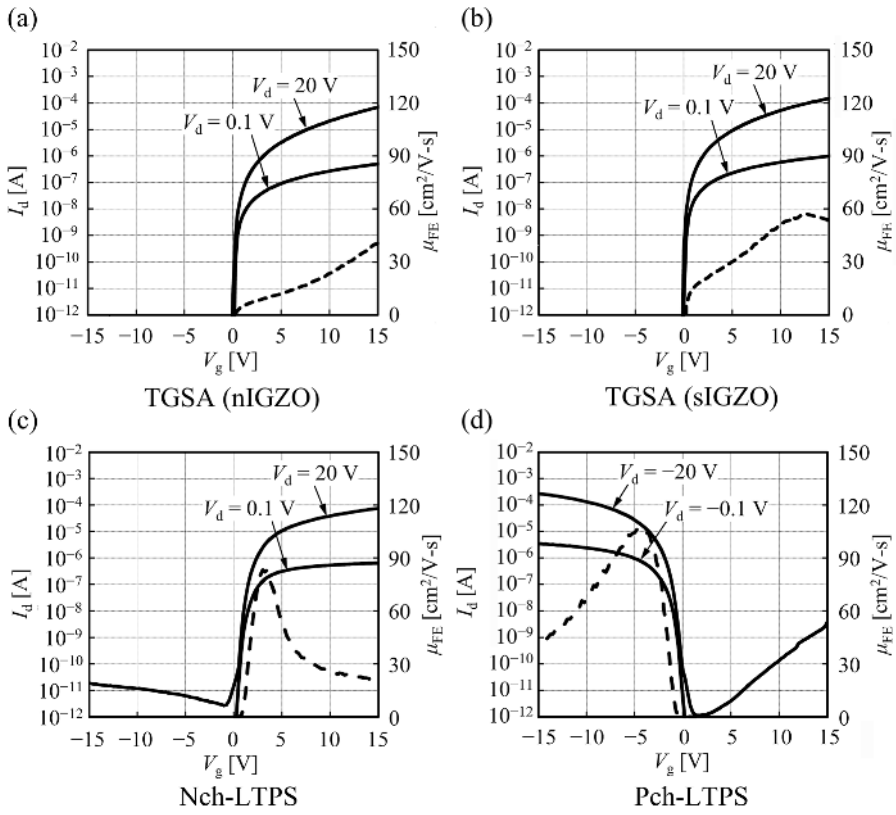

Figure 1.12 I_d–V_g characteristics of FETs with different semiconductor configurations. Measurement conditions: $V_g = -15$ to 15 V (0.25 V step), $V_d = 0.1$, 20 V, and $V_s = 0$ V (COMMON). Solid and dashed lines denote I_d–V_g and mobility (at $V_d = 20$ V) curves, respectively. The channel lengths (L) and widths (W) are (a) $L/W = 2/3$ μm, (b) $L/W = 2/3$ μm, (c) $L/W = 2.7 \times 2/3$ μm, and (d) $L/W = 3.2 \times 2/6.4$ μm. LTPS has two gates aligned parallel in the same plane, connected in series, each with a length of 2.7 μm in (c) and 3.2 μm in (d)

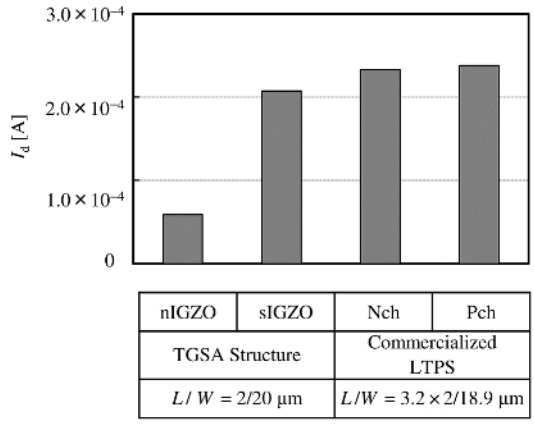

Figure 1.13 Comparison of the on-state current between FETs with different semiconductor layers ($|V_g| = 10$ V and $|V_d| = 5$ V)

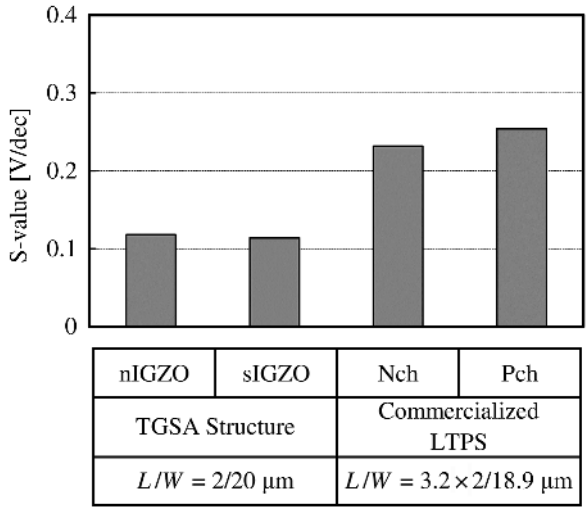

Figure 1.14 Comparison of *S*-values between FETs with different semiconductor layers ($|V_d| = 10$ V)

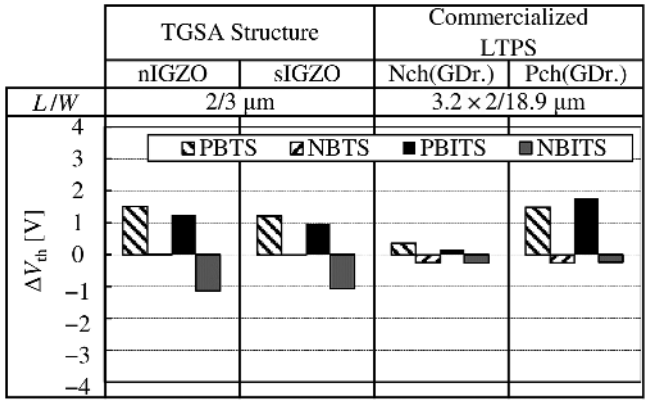

Figure 1.15 Results of the GBT stress tests of FETs with different semiconductor materials and structures. Test conditions: $V_g = \pm 30$ V and $V_d = V_s = 0$ V (COMMON); stress temperature 60 °C; application time of stress 1 h; dark/photo stress (pseudo-white OLED, 10,000 lx). PBTS, NBTS, PBITS, and NBITS stand for positive bias temperature stress, negative bias temperature stress, positive bias illumination temperature stress, and negative bias illumination temperature stress, respectively

and sIGZO FETs exhibited sufficient saturation even with a short channel length of $L = 2$ μm. This proved that CAAC-IGZO FETs are highly resistant to the short-channel effect, and thereby enabled FET size reduction. It also resulted in higher display resolutions and smaller footprints.

Lastly, the FET characteristic of the latest IGZO is presented in Figure 1.17. The latest IGZO has a mobility of a record of 100 cm^2/V-s or higher. Thus, in the near future, IGZO is expected to achieve a practical level with higher mobility than LTPS.

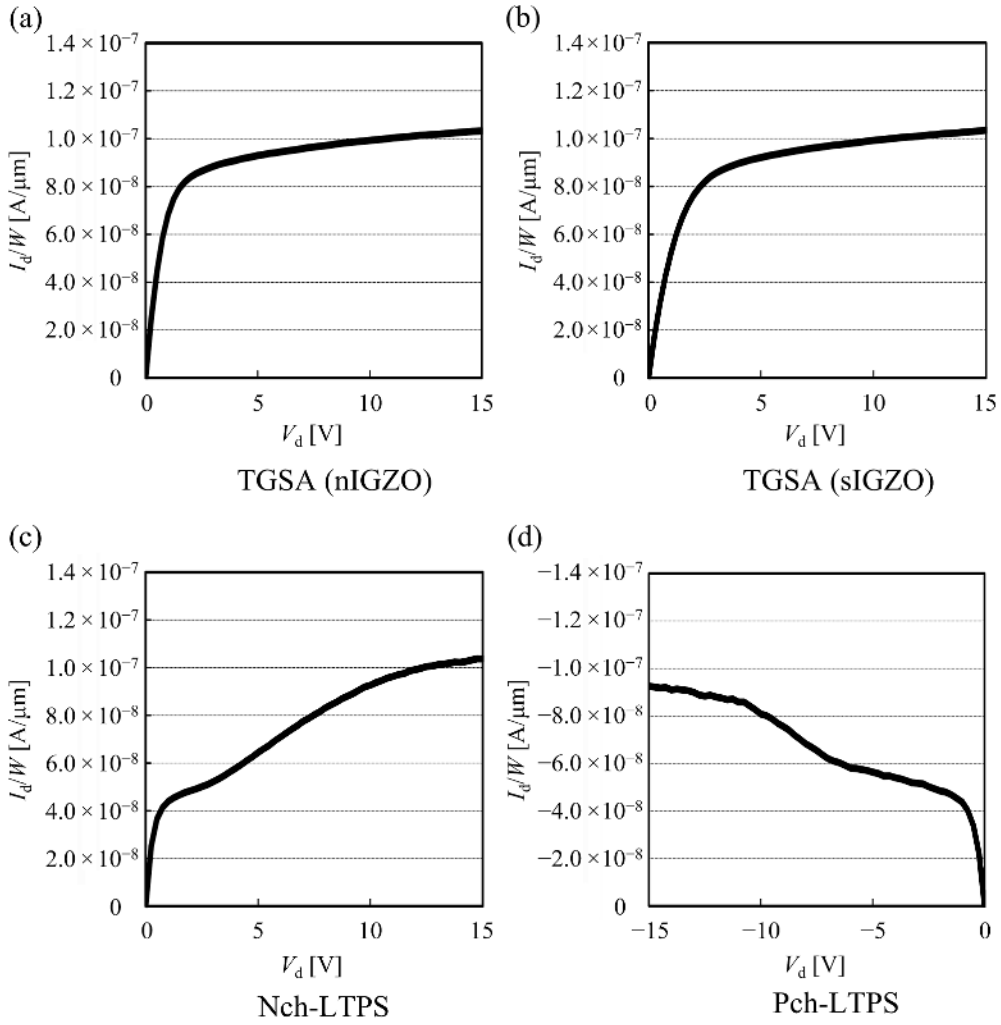

Figure 1.16 Comparison of the saturation characteristics of FETs with different semiconductor materials and structures. Measurement conditions: $I_d - V_d$: $V_d = 0$ to 15 V (0.25 V step); V_g is a voltage at which $I_d/W = 100$ nA/μm at $|V_d| = 10$ V; $V_s = GND$; room temperature; dark environment. The channel lengths (L) and widths (W) are as follows: (a, b): $L/W = 3/3$ μm, (c, d): $L/W = 3.2 \times 2/6.4$ μm. *Source*: Adapted from [23]. Reprinted with permission of Wiley

1.3.5 Development of OLED Displays

As described in the previous sections, CAAC-IGZO FETs have several advantages over Si TFTs. Therefore, displays are developed with CAAC-IGZO FETs to exploit these advantages. In particular, CAAC-IGZO matches the requirements of ultra-high-resolution OLED displays and flexible OLED displays for wearable devices. The details of these devices will be described in the following chapters. Figure 1.18 illustrates the current development status of the OLED

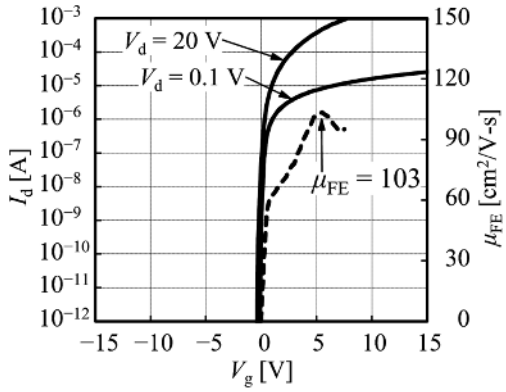

Figure 1.17 I_d–V_g characteristics of FETs with the latest IGZO

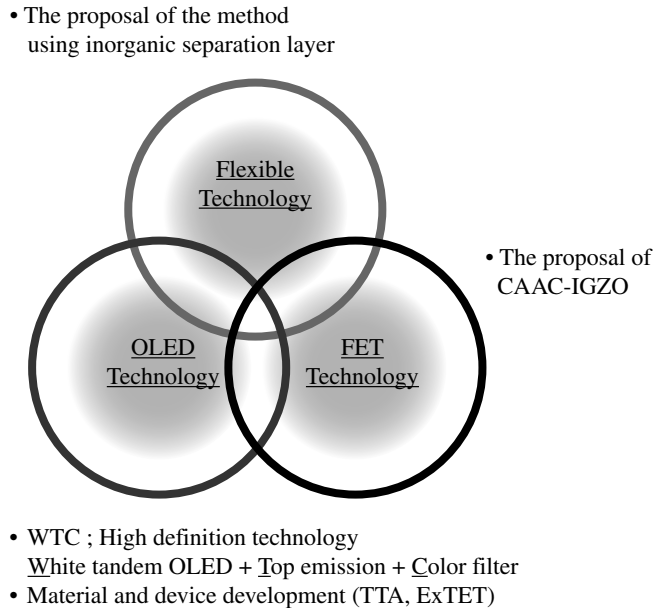

Figure 1.18 The developments for OLED displays

displays. The development of the OLED materials and FETs for a transfer process (see Chapter 5) to enable flexible display fabrication is currently in progress. As shown in Figure 1.19, the display resolution has increased steadily since 2012. This was also reported at various exhibitions and academic societies, including the Society for Information Display (SID) [24–28]. This volume offers an in-depth discussion of the fabrication of OLED displays reported at SID and elsewhere. The authors hope that the reader will find this information useful (see Chapters 4 and 5).

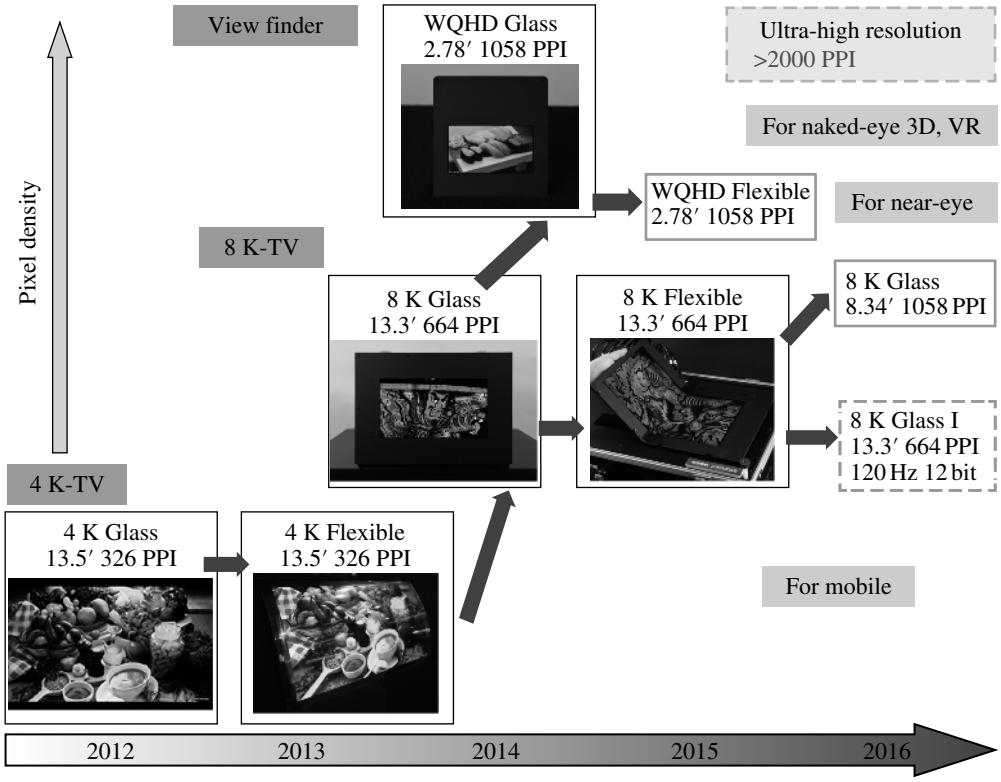

Figure 1.19 The transition timeline of the developments in OLED displays

Subsequent chapters explain the two types of CAAC-IGZO FET structure and their fabrication processes. This is followed by descriptions of the circuit designs for displays using CAAC-IGZO.

References

[1] Yamazaki, S. and Kimizuka, N. (in press) *Physics and Technology of Crystalline Oxide Semiconductor CAAC-IGZO: Fundamentals*. Chichester, UK: John Wiley.

[2] Yamazaki, S. and Fujita, M. (in press) *Physics and Technology of Crystalline Oxide Semiconductor CAAC-IGZO: Application to LSI*. Chichester, UK: John Wiley.

[3] Ukai, Y. (2007) *Thin Film Transistor*. Tokyo: Kogyo Chosakai Publishing [in Japanese].

[4] Lechner, B. J., Marlowe, F. J., Nester, E. O., and Tults, J. (1971) "Liquid crystal matrix displays," *Proc. IEEE*, **59**, 1566.

[5] Shishikui, Y. (2013) Research and Development of Super Hi-Vision. NHK Science & Technology Research Laboratories (STRL) R&D No. 137. Available at: www.nhk.or.jp/strl/publica/rd/rd137/PDF/P04-09.pdf [in Japanese].

[6] Sugawara, M. (2008) "Super hi-vision research on a future ultra-HDTV system," *EBU Tech. Rev*. Available at: tech.ebu.ch/docs/techreview/trev_2008-Q2_nhk-ultra-hd.pdf.

[7] le Comber, P. G., Spear, W. E., and Ghaith, A. (1979) "Amorphous-silicon field-effect device and possible application," *Electron. Lett.*, **15**, 179.

[8] Tsujimura, T. (2012) *OLED Display Fundamentals and Applications*. Chichester, UK: John Wiley.
[9] Oana, Y., Kotake, H., Mukai, N., and Ide, K. (1983) "Electrical properties of polycrystalline-silicon MOSFETs on glass," *Jpn. J. Appl. Phys.*, **22**(22-1), 493.
[10] Morozumi, S. (1989) "Poly-Si TFTs for large-area applications," *Japan Display.*, **89**, 148.
[11] Sameshima, T., Usui, S., and Sekiya, M. (1986) "XeCl excimer laser annealing used in the fabrication of poly-Si TFTs," *IEEE Electron Device Lett.*, **7**, 276.
[12] Serikawa, T., Shirai, S., Okamoto, A., and Suyama, S. (1989) "Low-temperature fabrication of high-mobility poly-Si TFTs for large-area LCDs," *IEEE Trans. Electron Devices*, **36**, 1929.
[13] Yamazaki, S., Hirohashi, T., Takahashi, M., Adachi, S., Tsubuku, M., Koezuka, J., *et al*. (2014) "Back-channel-etched thin-film transistor using *c*-axis-aligned crystal In–Ga–Zn oxide," *J. Soc. Inf. Disp.*, **22**, 55.
[14] Yamazaki, S., Zhang, H., and Ishihara, H. (1999) US Patent 6,002,101.
[15] Shinohara, H. and Sugawara, A. (1998) US Patent 6,149,988.
[16] Kubo, N., Kusumoto, N., Inushima, T., and Yamazaki, S. (1994) "Characteristics of polycrystalline-Si thin film transistors fabricated by excimer laser annealing method," *IEEE Trans. Electron Devices*, **41**, 1876.
[17] Yamazaki, S. (2014) "Future possibility of c-axis-aligned crystalline oxide semiconductor: Comparison with low-temperature polysilicon," *SID Symp. Dig. Tech. Pap.*, **45**, 9.
[18] Takahashi, K., Sato, T., Yamamoto, R., Shishido, H., Isa, T., Eguchi, S., *et al*. (2015) "13.3-inch 8k4k 664-ppi foldable OLED display using crystalline oxide semiconductor FETs," *SID Symp. Dig. Tech. Pap.*, **46**, 250.
[19] Shima, Y., Kanemura, H., Higano, S., Hosaka, Y., Okazaki, K., Koezuka, J., *et al*. (2015) "Channel-etched CAAC-OS FETs using multi-layer IGZO," *SID Symp. Dig. Tech. Pap.*, **46**, 1158.
[20] Toyotaka, K., Miyake, H., Kaneyasu, M., Yamashita, A., Jikumaru, M., Koyama, J., *et al*. (2014) "513-ppi liquid crystal display using c-axis aligned crystalline oxide semiconductor with narrow bezel and aperture ratio greater than 50%," *SID Symp. Dig. Tech. Pap.*, **45**, 634.
[21] Hatano, K., Chida, A., Okano, T., Sugisawa, N., Inoue, T., Seo, S., *et al*. (2010) "3.4-inch QHD flexible AMOLED with oxide TFT," *Proc. AM-FPD'10 Dig*., 263.
[22] Okazaki, K., Kanemura, H., Kurosaki, D., Shima, Y., Koezuka, J., Kawashima, S., *et al*. (2015) "Fabrication of 8k4k organic EL panel using high-mobility IGZO material," *SID Symp. Dig. Tech. Pap.*, **46**, 939.
[23] Shima, Y., Jincho, M., Hamochi, T., Saito, S., Dobashi, M., Okazaki, K., *et al*. (2016) "Development of a top-gate transistor with short channel length and c-axis-aligned crystalline indium–gallium–zinc-oxide for high-resolution panels," *SID Symp. Dig. Tech. Pap*., **47**, 1037.
[24] Tanabe, T., Amano, S., Miyake, H., Suzuki, A., Komatsu, R., Koyama, J., *et al*. (2012) "New threshold voltage compensation pixel circuits in 13.5-inch Quad full high definition OLED display of crystalline In–Ga–Zn-oxide FETs," *SID Symp. Dig. Tech. Pap.*, **43**, 88.
[25] Eguchi, S., Shinoda, H., Isa, T., Miyake, H., Kawashima, S., Takahashi, M., *et al*. (2012) "13.5-inch Quad-FHD top-emission OLED display using crystalline-OS-FET," *SID Symp. Dig. Tech. Pap.*, **43**, 367.
[26] Aoyama, T., Komatsu, R., Nakazato, R., Ohno, N., Jinbo, Y., Eguchi, S., *et al*. (2013) "13.5-inch Quadra-FHD flexible AMOLED with crystalline oxide FET," *Proc. AM-FPD'13 Dig*., 223.
[27] Kawashima, S., Inoue, S., Shiokawa, M., Suzuki, A., Eguchi, S., Hirakata, Y., *et al*. (2014) "13.3-in. 8 K × 4 K 664-ppi OLED display using CAAC-OS FETs," *SID Symp. Dig. Tech. Pap.*, **45**, 627.
[28] Yokoyama, K., Hirasa, S., Miyairi, N., Jimbo, Y., Toyotaka, K., Kaneyasu, M., *et al*. (2015) "A 2.78-in 1058-ppi ultra-high-resolution OLED display using CAAC-OS FETs," *SID Symp. Dig. Tech. Pap.*, **46**, 1039.